MICROWAVE PROPERTIES AND MODELING OF HIGH-T_c SUPERCONDUCTING THIN FILM MEANDER LINE*

A. Fathy, D. Kalokitis, V. Pendrick, E. Belohoubek
David Sarnoff Research Center, Princeton, NJ 08543

T. Venkatesan, L. Nazar, J. B. Barner
Bellcore, Red Bank, NJ 07701

A. Findikoglu, A. Inam, X. D. Wu, X. X. Xi and W. L. McLean
Rutgers University, Piscataway, NJ 08854

ABSTRACT

Meander lines have been utilized for the characterization of laser-deposited thin film high-T_c superconducting material. In this paper, we modeled the dispersion characteristics of the meander line and investigated the power dependence of high-T_c materials as a function of frequency and temperature. Measurements showed that magnetic fields as low as 0.1 Oe will affect the superconducting material decreasing the Q of the meander lines. The Q deterioration, is both temperature and frequency dependent and the latter is less pronounced at higher frequencies.

INTRODUCTION

We have utilized meander line resonators to characterize the properties of high T_c superconducting materials [1]. Our measurement scheme is well suited for the evaluation of superconducting thin film materials over wide temperature and frequency ranges. The material is evaluated under practical conditions, where effects such as deposition uniformity, sensitivity to chemical etchants, dielectric losses, and superconductor/dielectric interface losses are all included (see Fig.1 for a sketch of the test set-up).

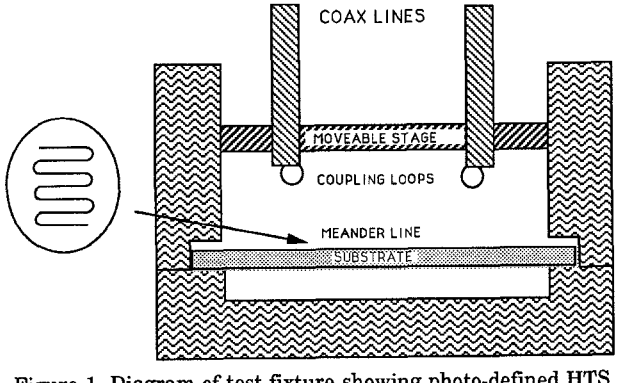

Figure 1. Diagram of test fixture showing photo-defined HTS meander line on one surface of the lanthanum aluminate substrate. A gap is provided below the substrate to minimize the effects of the normal metal ground plane.

We have measured the unloaded-Q, of patterned high quality laser deposited YBaCuO thin film meander lines, up to 20 GHz. Unloaded-Q was measured through the use of a very loose coupling scheme. We measured surface resistance values as low as 0.5 mΩ, for laser deposited 123 films on $LaAlO_3$, at 10 GHz and 79K [2]. The Sarnoff/ Bellcore surface resistance data, at 77K, follow approximately f^2 frequency dependence as shown in Fig. 2.

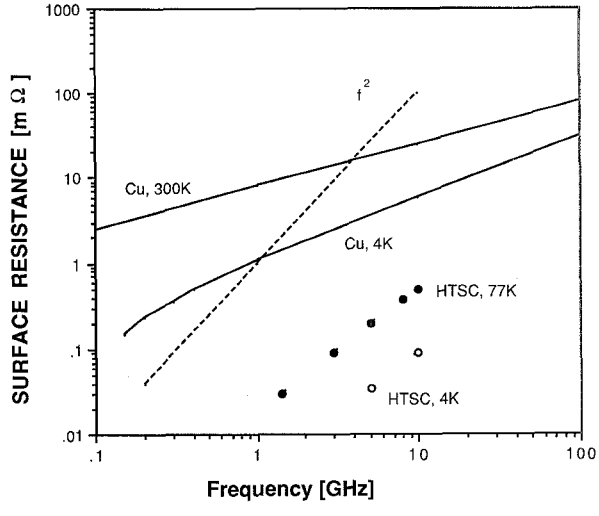

Figure 2. The measured surface resistance data from 1 to 10 GHz exhibits approximately f^2 frequency dependence.

The surface impedance of the superconducting material is not zero, and a non-vanishing rf electric field component will exist at the superconductor surface due to the Cooper pair's inertia. Consequently, for a two conductor transmission line, the lowest mode is not a TEM mode but a TM mode. The complex propagation constant of the electromagnetic waves along these lines will depend on both the real and imaginary parts of the complex surface impedance Z_s and the finite thickness t of the superconducting thin films as given by [3]:

$$Z_s = \sqrt{j\omega\mu/\sigma}\,\coth\sqrt{j\omega\mu\sigma}\,t, \qquad (1)$$

where σ is the complex conductivity.

* This work was partially supported by the Strategic Defense Initiative Organization under Contract SDIO 84-88-C-0044.

To evaluate the dispersion of these meander lines, we have modeled the meander line by a simple equivalent circuit consisting of n-parallel coupled transmission lines of width w and spacing s. The lines are connected at alternating ends by transmission lines of length s, and coupling is assumed to exist only between these n-parallel lines. For inhomogeneous structures, such as microstrip lines or suspended substrate structures, the stopbands are due to the difference in the phase velocities of the even and odd modes of a typical normal mode of that structure, as well as the effect and location of the connecting lines between the different parallel lines [4].

In this paper, we present the results of this dispersion investigation, and our measurement/ analysis of the power dependence of the high-T_c superconducting material as a function of frequency and temperature. The rf magnetic field and current effects on the measured Q-values will be discussed in detail.

MODELING OF THE MEANDER LINE

The forward transmission coefficient for the meander line and the coupling structure has maximum values whenever the total line length is a multiple of a half wavelength. The measured separation between successive peaks in the transmission coefficient is not uniform. The separation is smallest near the center frequency and increases in both directions as one moves further away from it, as shown in Fig. 3. An analysis of the meander line including the line periodicity and the coupling effects between adjacent line segments has been carried out. The line is dispersive, which is of no consequence for the measurement of the surface resistance, but would be important if the meander line were to be used as a wide band delay line.

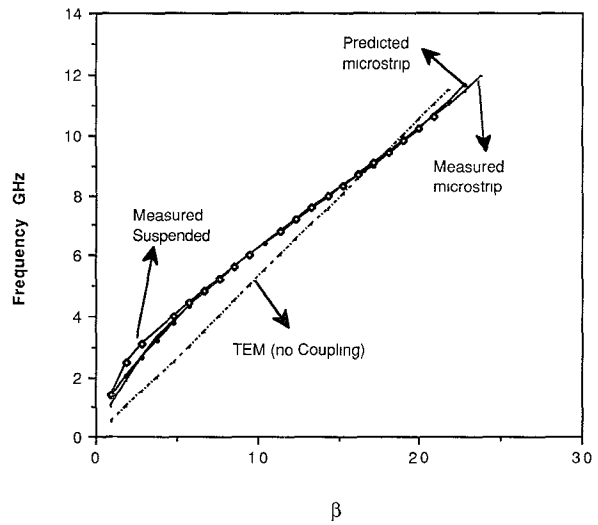

Figure 3. The ω–β diagram for microstrip and suspended substrate meander line structures (β in rad/inch).

The microstrip meander line is represented by 29-coupled lines of length l=0.100", width w=.001", and spacing s=0.010", and the links are 0.001" wide lines and 0.010" long. The dielectric substrate has a thickness of 0.020" and a dielectric constant of ε_r=25. The propagation constant β (β=nπ/L where n is the harmonic number, and L is the total meander line length) and the resonant frequencies f_o were calculated and compared to the measured results of the high T_c meander line microstrip structure. Good agreement was observed between predicted and measured results as shown in Fig. 3.

The meander line used for R_s measurements has a 50 mil air gap beneath the substrate as seen in Fig.1, in order to reduce the losses from the normal metal ground plane. However, in a practical implementation of a non-dispersive delay line, it would be necessary to use two superconducting ground planes spaced at a distance smaller than the line spacing s in a symmetrically loaded structure such as a stripline.

The measured resonant frequencies are temperature dependent. A noticeable frequency drift to higher values was measured if operated at lower temperatures, especially when using films with thicknesses comparable to the London penetration depth λ. This shift is related to the temperature dependence of the phase velocity v_ϕ, and is empirically given by [3]:

$$v_\phi = 1/\sqrt{\mu\varepsilon_o\varepsilon_{eff}}\,(1+\kappa\,\lambda/h\,\coth\,t/\lambda)^{-1/2} \qquad (2)$$

where ε_o is the permittivity, μ is the permeability, ε_{eff} is the effective dielectric constant of the suspended substrate structure, and h is the dielectric substrate height. κ is a geometric factor which accounts for the use of a very small w/h suspended substrate structures [5]. The temperature dependence of London penetration depth λ according to Gorter and Casimir's two-fluid model is given by [5]:

$$\lambda(T)=\lambda(o)/\sqrt{1-(T/T_c)^4} \qquad (3)$$

Excellent curve fitting was obtained at f=3.15 GHz, as seen in Fig.4, where T_c, and t were 91K, and 5000A° respectively, and λ(o) was taken to be 1500A°.

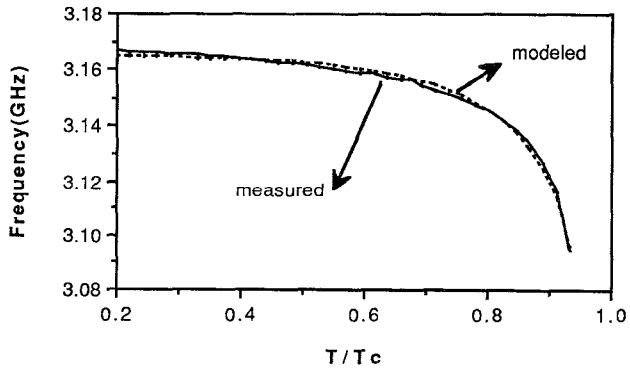

Figure 4. Predicted and measured temperature dependence of resonant frequency.

Currently, we are extending the previous curve fitting to other harmonic frequencies as well, in order to have a better estimate for the values of T_c, $\lambda(o)$, and κ over wide temperature and frequency ranges.

POWER DEPENDENCE

To explore the Q reduction that occurs at lower frequencies, we measured the Q-values of the meander line as a function of frequency and source input power. The meander line is clearly power limited as illustrated in Fig. 5. Since the knowledge of the maximum tolerable power levels is crucial for many applications, additional measurements were performed. We took a separate set of measurements covering a wide range of input powers, at several frequencies and different temperatures.

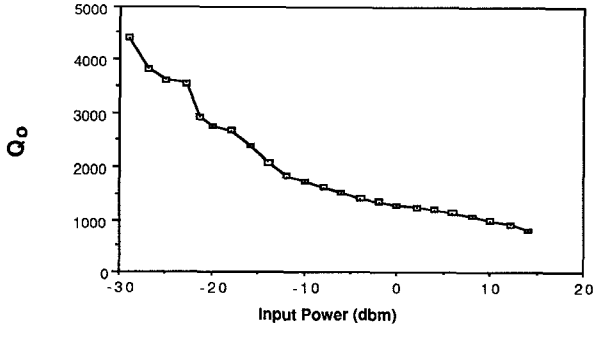

Figure 5. Q as a function of input power, f=3 GHz, T=79K.

For a specific resonant frequency, the input power to the meander line, the Q of the meander line, and the net transmission coefficient S_{21} through the resonator were measured. The temperature and mechanical coupling structure were held constant during these measurements. Data were taken at 79K, 72K, and 69K for the 1.4, 2.5, 6, and 8 GHz resonances.

A Fabry Perot resonator model was used to approximately estimate the EM fields in and out of this resonant structure [6]. Based on the maximum transmission coefficient S_{21} and the measured loaded Q_l , we can evaluate the attenuation coefficient of the line α and the reflection coefficient ρ due to the line-end discontinuity at both ends, as given by

$$S_{21}{}^2{}_{max}=\left|\frac{(1-\rho^2)e^{-\alpha L}}{(1-\rho^2 e^{-2\alpha L})}\right|^2, \qquad (4)$$

$$\text{and } Q_l=\frac{\beta}{2\alpha}, \qquad (5)$$

where β (the propagation constant of the electromagnetic wave along the meander line) is determined from the coupled line model that was used to study the meander line dispersion previously, and Q_l is calculated using the 3-dB points of the transmission coefficient S_{21}.

Approximate analytical expressions were derived to relate the input power to the maximum electric and magnetic fields along the meander line. Basically, there is a standing wave pattern along the meander line whose magnitude is proportional to Q. A Quasi-TEM mode is assumed with the electric field E perpendicular, and the magnetic field H tangential to the conducting line, both in the transverse plane. The current crowding effects, and the loss of the coupling structure were neglected. Multiple reflections were used to evaluate the tangential magnetic field component H at any point (z_1) along the line, leading to:

$$H(z_1)=\sqrt{1-\rho^2}\,\frac{E_i}{Z_o}\,e^{-\alpha z_1}\cdot\frac{(1-\rho e^{-2j\beta(L-z_1)}e^{-2\alpha(L-z_1)})}{(1-\rho^2 e^{-2j\beta L}e^{-2\alpha L})}, \qquad (6)$$

where $0< z_1<L$, E_i is the incident electric field given in volt/m, and the characteristic impedance of the line is Z_o. The electric field is related to the incident power P_i in Watts by $E_i=\sqrt{2P_i Z_o/(wh)}$, where w and h are the effective strip width and the substrate height respectively. The maximum magnetic field and the maximum current can then be approximately calculated for the various n harmonics at $z_1=L/2n$, where n is the harmonic number. Figures 6, 7, 8, and 9 show the measured 1/Q, where 1/Q is approximately proportional to R_s versus the corresponding maximum rf magnetic field values calculated.

It is evident that magnetic fields as low as 0.1 Oe will affect the superconducting material, and the Q-deterioration is both temperature and frequency dependent. The surface resistance increases approximately linearly with the magnitude of the applied magnetic field with a weak temperature dependence. Measurements at higher frequencies also show a linear dependence on magnetic field strength, but show an increase of nearly an order of magnitude in the critical field values and less sensitivity to the applied rf fields (see Fig. 9). The magnetic field is related to the surface current J_s, flowing along the meander line. Figure 10 shows a sample calculation for f= 8 GHz where currents in the order of $10^5 A/cm^2$ can be seen to exist on the line.

The current thin film superconducting material, apparently, has a low critical field H_{c1} at which the flux first penetrates the material, and the surface resistance increases linearly from there with the applied magnetic field. According to Ref. [7] this may be explained as follows: as the field exceeds H_{c1} the material admits individual flux quanta in vortices. At low fields the vortex cores occupy a negligible fraction of the total volume, but at high fields, the entire superconductor will be full of these cores leading to a transition to the normal state (within the rf magnetic field values applied, we have not seen this transition in our measurements). Flux penetration in the presence of a transport current may cause higher dissipation, because when a transport current passes through a superconductor in this state, a Lorentz force will act on these vortices and at the same time, chemical or physical defects in the superconductor exert forces on the vortices to keep them trapped or "pinned" at the locations of these defects. If the Lorentz forces exceed the pinning forces, the vortices move, leading to a higher

surface resistance and dissipation. To improve the power handling capability of thin films special attention will have to be given to vortex pinning, similarly to what has been done previously for low temperature superconductors.

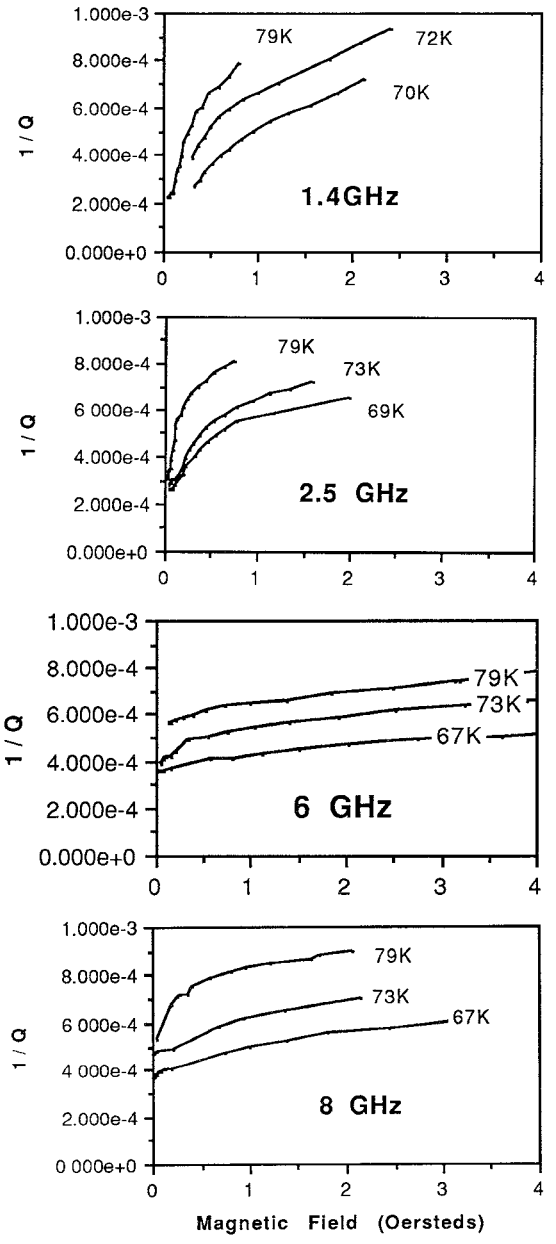

Figure 6-9. Measured 1/Q response of meander line at various frequencies vs magnetic field corresponding to applied rf power level. Coupling effects have been removed allowing true incident power on the line to be evaluated. The 1/Q values for an equivalent Cu line were measured and decrease as $1/\sqrt{f}$ between .03 and .01 at 1 and 10 GHz respectively and 77K.

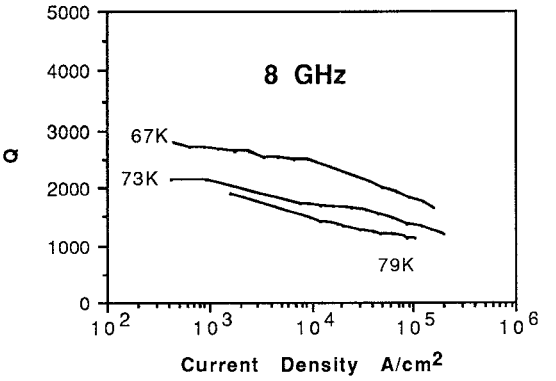

Figure 10. Measured Q vs current density on the line corresponding to incident rf power level.

CONCLUSIONS

The meander line measurement technique is ideally suited for characterizing the power dependence of high-T_c materials as a function of frequency and temperature. The meander line dispersion was modeled taking the periodicity and the coupling into account. Using the meander line as a Fabry Perot resonator, we found that magnetic fields as low as 0.1 Oe will affect the superconducting material and the Q deterioration is both temperature and frequency dependent. Higher power levels can be tolerated at higher frequencies

REFERENCES

1. D. Kalokitis et al., "Measurement of Microwave Surface Resistance of Superconducting Thin Films," J. of Electronic Materials, Jan. 1990, pp. 117-121.
2. E. Belohoubek et al., "Microwave Measurements on Patterned High Temperature Superconducting Thin Film Circuits," Proceedings SPIE Symposium, Santa Clara, Oct. 12, 1989.
3. R. L. Kautz, "Picosecond pulses-on superconducting striplines," J. Apl. Phys. 49(1), Jan 1978, pp. 314-308.
4 J. A. Weiss, "Dispersion and Field Analysis of a Meander-Line Slow-Wave Structure," IEEE Trans. Microwave Theory Tech., vol. MTT-22, Dec. 1974, pp. 1194-1201.
5 V. L. Newhouse, **Applied Superconductivity**. New York: John Wiley and Sons 1964, pp. 103-105.
6. J. Verdeyen, **Laser Electronics**, Prentice Hall, Inc. 1981, pp. 112.
7. Van Duzer, and C. W. Tuner, "**Principles of Superconductive Devices and Circuits**," Elsevier North Holland, Inc., 1981, chapter 8